Design of Pd/B_4C aperiodic multilayers for 8–12 nm region with flat reflectivity profile

Yiwen Wang (王轶文)[1], Qiushi Huang (黄秋实)[1], Qiang Yi (易 强)[1,2], Li Jiang (蒋 励)[1], Zhong Zhang (张 众)[1], and Zhanshan Wang (王占山)[1,*]

[1]*Key Laboratory of Advanced Micro-Structured Materials MOE, Institute of Precision Optical Engineering, School of Physics Science and Engineering, Tongji University, Shanghai 200092, China*

[2]*Institute of Nuclear Physics and Chemistry CAEP, Mianyang 621900, China*

**Corresponding author: wangzs@tongji.edu.cn*

Received February 4, 2016; accepted May 16, 2016; posted online June 13, 2016

The Pd/B_4C multilayer is a promising candidate for high reflectance mirrors operating in the 8–12 nm extreme ultraviolet wavelength region. To extend the working bandwidth beyond the L-edge of silcon, we theoretically design broadband Pd/B_4C multilayers. We discuss the influence of the desired reflectance of the plateau, number of bilayers, and the real structural parameters, including the interface widths, layer density, and thickness deviation, on the reflectivity profile. Assuming the interface width to be 0.6 nm, we design aperiodic multilayers for broad wavebands of 9.0–10.0, 8.5–10.5, and 8.0–11.0 nm, with average reflectivities of 3.1%, 5.0%, and 9.5%, respectively.

OCIS codes: 310.4165, 230.4170, 340.7480, 350.1270.
doi: 10.3788/COL201614.073101.

High reflectivity multilayer mirrors are widely required in the applications of x-ray and extreme ultraviolet (EUV) astronomy, EUV photo-lithographs accelerator-based light sources, and x-ray plasma diagnostics[1–5]. Among these applications, the 8-12 nm wavelength region is of particular interest. It contains many characteristic emission lines of the multiple-charged ions of different elements, like iron (Fe), magnesium (Mg), and silcon (Si), which are very important for solar observation and deep space exploration in the EUV region[6]. The working wavelengths of the EUV free election lasers also include this range[7]. Thus, high reflectivity multilayer mirrors are demanded in this wavelength region. Moreover, for wideband EUV spectroscopy or high resolution imaging with a large numerical aperture, broad spectral or angular responses are required for a single mirror. In these cases, an aperiodic multilayer with a varied layer thickness over the stack is needed[8–15]. As the wavelength is below the Si L-edge ($\lambda = 12.4$ nm), the widely used Mo/Si multilayer cannot be used anymore. Mo/Y has been applied in this region for normal incidence mirrors and polarizers, due to its stable layer structure[16–18]. However, the theoretical reflectivity of a periodic Mo/Y multilayer is less than 50% at $\lambda = 9.5$ nm, and the experimentally achieved reflectivity was only 38.4%[18]. To achieve a higher reflectivity, new material combinations, like Ag/Y, Pd/Y, Ru/Y, Rh/Y, Pd/B_4C, etc, have been proposed and studied recently for the 8-12 nm region[3,19–21]. Based on these materials, the maximum theoretical reflectivity of a periodic multilayer is above 60% at 9.5 nm. The designed wideband multilayers exhibit a high average reflectivity of 11.5% and 11.4% over the 9-13 nm range by using Ag/Y and Pd/Y, respectively[19]. However, the physical structure of Ag/Y and Pd/Y is unstable, which provides a very low experimental reflectance that cannot be used in applications[22]. Although the Pd/Y multilayer structure has been improved by using interface engineering methods, including using the barrier layers or passivation with nitrogen[20,23], the fabrication process is complicated. On the other hand, the Pd/B_4C multilayer possesses both a high theoretical reflectivity and stable layer structure. A high experimental reflectance of 43% was obtained at 9.1 nm using the periodic multilayer at a near normal incidence[3]. An aperiodic Pd/B_4C multilayer was also designed with an average reflectivity of 8.8% from 9 to 13 nm[19]. It is indicated that Pd/B_4C is a promising multilayer mirror for the wideband applications. To fully explore the wideband performance of this multilayer, the effects of different structural factors, the fabrication inaccuracy, and the different bandwidths on the reflectivity profile need to be studied, which were absent in the former work. Thus, in this Letter, we performed a systematic design of the aperiodic Pd/B_4C multilayers for the 8–12 nm waveband, including the optimization and discussion of different factors. Flat reflectivity profiles with the average reflectivity of 9.5%, 5.0%, and 3.1% are designed over the wavebands of 9.0–10.0, 8.5–10.5, and 8.0–11.0 nm, assuming the interface widths of 0.6 nm.

The design of the broadband Pd/B_4C multilayers consists of two steps. First, we optimize and determine a proper initial multilayer structure based on the power law structure[24]. The layer thickness distribution in the initial structure follows the formula $d = a/(b + j)^c$, where j is the layer index (from top to bottom), and d_j is the j-th layer thickness. To obtain a flat reflectivity profile, a, b, and c are optimized through the minimization of the merit function,

$$\mathrm{MF}\sum_{i=1}^{M}[R(i)-R_0]^2, \tag{1}$$

using the genetic algorithm[25]. In the merit function, $R(i)$ is the reflectivity at the ith wavelength position, $R_0(i)$ is the desired constant reflectivity of the plateau, and M is the number of points calculated over the spectral region. Second, we optimize each layer thickness of the multilayer structure with a local minimization algorithm to reduce the oscillation of the reflectivity profile. In order to obtain a relatively smooth thickness distribution, the thickness variation of different layers was restricted during the optimization[26]. The minimum layer thicknesses of Pd and B_4C are set as ≥1 nm to keep a continuous layer growth in fabrication. The optical constants of the materials were obtained from the x-ray database of the Center for X-ray Optics[27].

To find the maximum reflectivity with a flat profile, we first analyzed the effect of the desired reflectivity of the plateau and the number of bilayers during optimization. With absorption-free materials, an aperiodic multilayer can, in theory, achieve almost 100% reflectivity over the broad wavelength range[28]. However, due to the absorption of all materials, the real aperiodic multilayer has a limited maximum reflectivity which needs to be explored for different wavebands. Here, we studied the multilayer designed for the waveband of 8.5–10.5 nm with a fixed number of bilayers of 120 and different desired reflectivities of the plateau (R_0) of 8%, 9%, 10%, 12%, and 14%, respectively. The incidence angle is 5 degrees off normal. As shown in Fig. 1, with the desired reflectivity set as 8%, the designed reflectivity profile is very flat. The mean reflectivity is 7.94% and the standard deviation,

$$D_{\mathrm{standard}}=\sqrt{\sum_{i=1}^{N}(R_i-R_{\mathrm{average}})^2/N}, \tag{2}$$

is only 0.04%. As R_0 increases to 9%, the mean reflectivity increases to 8.61%, and the standard deviation is enlarged to 0.14%. Further increasing R_0 only improves the reflectivity at part of the waveband, and the oscillation of the

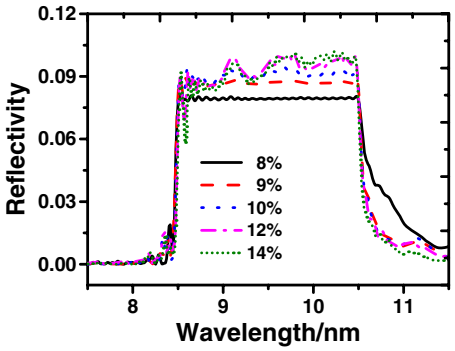

Fig. 1. Designed reflectivity profiles of aperiodic Pd/B_4C multilayers operating in the 8.5–10.5 nm waveband with different desired reflectivities.

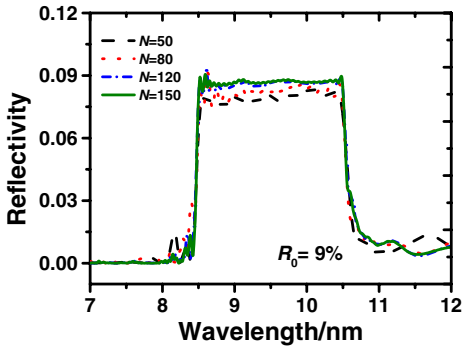

Fig. 2. Designed reflectivity profiles of aperiodic Pd/B_4C multilayers operating from 8.5 to 10.5 nm with a different number of bilayers.

reflectivity is enlarged. Thus, the desired reflectivity of 9% is the optimum value to achieve both a high reflectivity and flat profile for the waveband of 8.5–10.5 nm.

The number of bilayers will affect the designed performance since more bilayers can increase the reflectivity and smooth the profile until it is saturated. However, more bilayers also increase the difficulty of fabrication. To find the proper bilayer number, the aperiodic multilayer intended for the waveband of 8.5–10.5 nm is designed as an example, with 50, 80, 120, and 150 bilayers, respectively. The desired reflectivity is fixed to be 9%. The optimized reflectivity profiles are shown in Fig. 2. For the multilayer with 50 bilayers, the average reflectivity is only 7.91% with a 0.27% standard deviation. The profile has an obvious zigzag oscillation. A larger number of bilayers improves the reflectivity profile, and the multilayer with 120 bilayers provides an average reflectivity of 8.61% with a standard deviation of only 0.14%. Continuing to increase the bilayer number to 150 brings negligible improvement to the reflectivity profile. Considering both the broadband performance and the fabrication difficulty, the optimum number of bilayers is set as 120.

Besides the optimum desired reflectivity and the number of bilayers, we analyzed the effect of other structural factors determined by the fabrication process in order to make the experimental performance close to the designed one. These factors include the interface widths, layer density, and layer thickness deviation. The interface width, including both roughness and intermixing, will cause an obvious drop of the reflectance. It can also cause oscillation of the reflectivity profile. To study this effect, we designed an ideal Pd/B_4C aperiodic multilayer first with 120 bilayers and a bandwidth of 8.5–10.5 nm. Afterward, the interface width (σ) was taken into account at each interface of the multilayer by modifying the Fresnel reflection coefficient with the corresponding interface profile function, and the resulted reflectivity profile is calculated[29]. No interlayer was included in the structure model. According to the previous experimental results[21], the interface widths between Pd and B_4C were set as 0.6 nm, and the error function was used as the interface profile function. As shown in Fig. 3, the average reflectivity over

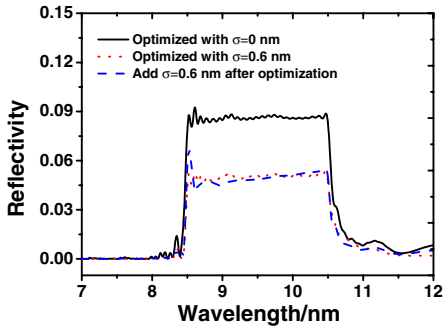

Fig. 3. Reflectivity profile of the aperiodic Pd/B_4C multilayer optimized with no interface width (solid), adding 0.6 nm interface width after optimization (dash), and optimized with the fixed interface width of 0.6 nm (dash dot).

the whole band is significantly decreased from 8.61% to 4.96% after the introduction of the interface widths. Moreover, there is one sharp peak appearing at the left edge of the plateau, and the reflectivity gradually increases with longer wavelengths. On the other hand, we designed the aperiodic multilayer with fixed interface widths of 0.6 nm in the model. The resulted reflectivity profile displays an average reflectivity of 5.03% with a very flat plateau, as shown in Fig. 3. It is evident that to achieve the flat reflectivity profile experimentally, the interface widths should be included during the design of the multilayer.

The real layer density is another factor that affects the experimental reflectance profile since it changes the optical constants of the layer. To analyze this factor, we first designed the aperiodic multilayer intended for the waveband of 8.5–10.5 nm using the bulk density of Pd and B_4C (100% density), $\rho_{pd} = 12.02$ g/cm^3, $\rho_{B4C} = 2.52$ g/cm^3, with 120 bilayers and 0.6 nm interface widths. As the density of the nanoscale thin films fabricated by magnetron sputtering is usually a little lower than the bulk value[30], the reflectance profile of the designed multilayer was then calculated using the layer densities of 95% and 90% of the bulk value for both Pd and B_4C. As shown in Fig. 4, the average reflectivity decreases from 5.03% to 4.75% and 4.46% as the density reduces to 95% and

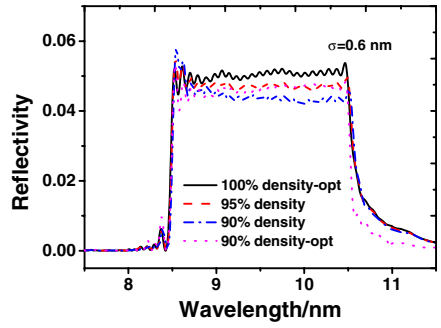

Fig. 4. Reflectivity profile of the original aperiodic multilayer optimized with 100% bulk density (solid), the original multilayer calculated with 95% (dash) and 90% bulk density (dash dot), and the multilayer optimized with 90% bulk density (dot).

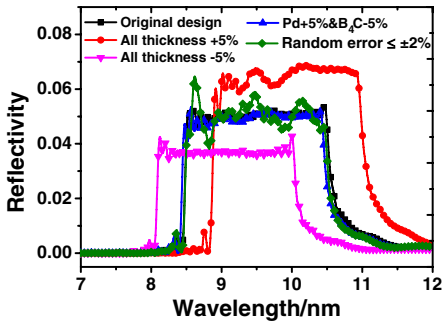

Fig. 5. Reflectivity profiles of the designed aperiodic multilayer with different layer thickness errors. The multilayer is designed for the waveband of 8.5–10.5 nm.

90%, respectively. Meanwhile, the flatness of the reflectivity profile is degraded compared to the original design, and it becomes worse with lower density. The distortion of the reflectivity profile can also be avoided by including the real layer density in the design. The aperiodic multilayer optimized with a 90% layer density displays a flat reflectivity profile with an average value of 4.62%. The slightly reduced reflectivity can be caused by the smaller difference of the optical constants between Pd and B_4C as the density decreases. However, the densities of the deposited Pd and B_4C layers were not characterized in detail in the former work. Thus, we still use the bulk density values in the following design and discussion.

The deviation of the deposited layer thicknesses from the designed values is the main factor in experiments that distorts the reflectivity profile. The layer thickness error can be divided into two types, the systematic error and the random error, which can be caused by the imperfect calibration of the deposition rate of Pd and/or B_4C and the instability of the process. We used the multilayer optimized for the waveband of 8.5–10.5 nm with 120 bilayers and 0.6 nm interface widths as the reference, as shown in Fig. 5. The layer thickness distribution of the multilayer is shown in Fig. 6. The variation of the layer thicknesses is small (except the top and bottom layer in the stack), which is relatively easy for the fabrication. The thicknesses of all layers were first increased or decreased by

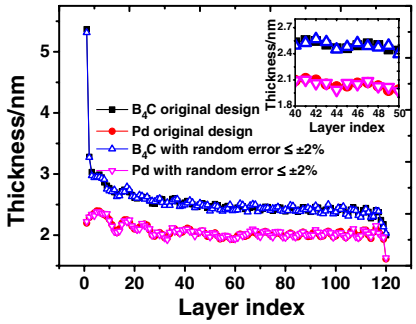

Fig. 6. Layer thickness distribution of the multilayer designed for the waveband of 8.5–10.5 nm (solid) with 120 bilayers, and the multilayer with random errors of $\leq \pm 2\%$ (open).

5% to study the effects. In these cases, the whole reflectivity profile shifts towards the longer or shorter wavelengths, respectively, while the bandwidth remains similar. Nevertheless, the average reflectivity increases as the plateau shifts to the longer wavelengths. This can be explained by the larger difference between the optical constants of Pd and B_4C as the wavelength increases, which is essential to obtain a high reflectance broadband multilayer. On the other hand, we increased and decreased the thicknesses of the Pd and B_4C layers by 5%, respectively and vice versa, while the total thickness of each bilayer remained unchanged. The resultant reflectivity profiles are very similar to the original one with a slight shift of the wavelength positions of the plateau due to the different refractive index between Pd and B_4C. For clarity of the figure, only one of the two results is displayed in Fig. 5. The random thickness errors of no more than ±2% were also introduced for all layers, and the changed thickness distribution is shown in Fig. 6. It can be seen that the small random errors already induce a significant oscillation at the reflectivity plateau. Moreover, these errors are more difficult to correct compared to the systematic errors in the fabrication. Thus, the random errors are the most sensitive thickness errors that need to be reduced during the iterative calibration and deposition experiments.

Based on the discussion above, we designed aperiodic Pd/B_4C multilayers with a working waveband of 9.0–10.0, 8.5–10.5, and 8.0–11.0 nm assuming 0.6 nm interface widths. The incidence angle is 5 degrees from normal, and the number of bilayers is 120. We used different desired reflectivities for the different bandwidth. The optimized reflectivity profiles are shown in Fig. 7, and the reflectivity of a periodic Pd/B_4C multilayer with a 0.6 nm interface width is also shown as a comparison. The periodic multilayer shows a peak reflectivity of 46.7%, but with only a 0.3 nm bandwidth in full width at half-maximum (FWHM). For the aperiodic multilayers intended for the waveband of 9.0–10.0, 8.5–10.5, and 8.0–11.0 nm, the average reflectivity of the plateau is 3.1%, 5.0%, and 9.5% with standard deviations of 0.29%, 0.08%, and 0.13%, respectively. The optimized bandwidths are 3–10 times larger than the periodic multilayer. The

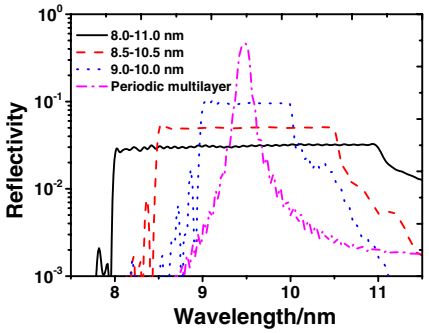

Fig. 7. Reflectivity profiles of the periodic Pd/B_4C multilayer and aperiodic multilayers designed for different bandwidths.

Table 1. Parameters of Optimization and the Resulted Reflectivity Profiles for Aperiodic Multilayers with Different Bandwidths

Waveband (nm)	Bilayer number N	Desired reflectivity (%)	Average reflectivity (%)	Deviation (%)
8.0–11.0	120	3.5	3.1	0.29
8.5–10.5	120	5.5	5.1	0.08
9.0–10.0	120	10.0	9.5	0.13

parameters of the optimization and the reflectivity profiles are listed in Table 1. The integral reflectivity over the bandwidth of the aperiodic multilayer is also larger than that of the periodic one. For the multilayer with an 8.5–10.5 nm waveband, the integral reflectivity is ~20% larger than that of the periodic one. The enhancement of the integral flux can be further improved by changing the merit function.

In conclusion, we perform a systematic design of the broadband Pd/B_4C multilayers operating at the region of 8–12 nm. Different factors that can influence the reflectivity profile are studied theoretically. To obtain the maximum reflectivity with a flat response over the bandwidth, the desired reflectivity and number of bilayers need to be optimized. The real structural parameters, including the interface width and layer density, can reduce the average reflectivity and degrade the flatness of the plateau that should be considered in the design. The random thickness error is a sensitive factor to the flatness of the plateau which needs to be controlled down to $< \pm 2\%$ in experiments. Based on this, we designed the broadband multilayers intended for different bandwidths assuming 0.6 nm interface widths. An average reflectivity of 3.1% for 8.0–11.0 nm, 5.0% for 8.5–10.5 nm, and 9.5% for a 9.0–10.0 nm waveband is demonstrated in theory, with a very flat reflectivity profile. These aperiodic Pd/B_4C multilayers can be easily fabricated and used for broadband imaging and spectroscopy applications.

This work was supported by the National Natural Science Foundation of China (Nos.11443007 and 11505129), the NSAF (No. U1430131), the National Key Scientific Instrument and Equipment Development Project (Nos. 2012YQ13012505 and 2012YQ24026402), and the Shanghai Pujiang Program (No. 15PJ1408000).

References

1. P. Boerner, C. Edwards, J. Lemen, A. Rausch, C. Schrijver, R. Shine, L. Shing, R. Stern, T. Tarbell, A. Title, C. J. Wolfson, R. Soufli, E. Spiller, E. Gullikson, D. McKenzie, D. Windt, L. Golub, W. Podgorski, P. Testa, and M. Weber, Solar Phys. **275**, 41 (2012).
2. E. Louis, A. E. Yakshin, T. Tsarfati, and F. Bijkerk, Prog. Surf. Sci. **86**, 255 (2011).
3. A. J. Corso, P. Zuppella, D. L. Windt, M. Zangrando, and M. G. Pelizzo, Opt. Express **20**, 8006 (2012).

4. S. Yi, B. Mu, J. Zhu, X. Wang, W. Li, Z. Wang, P. He, W. Wang, Z. Fang, and S. Fu, Chin. Opt. Lett. **12**, 083401 (2014).
5. S. Yi, B. Mu, X. Wang, L. Jiang, J. Zhu, Z. Wang, P. He, Z. Fang, W. Wang, and S. Fu, Chin. Opt. Lett. **12**, 093401 (2014).
6. M. Lorenc, M. Rybanský, and I. Dorotovič, Solar Phys. **281**, 611 (2012).
7. W. A. Ackermann, G. Asova, V. Ayvazyan, A. Azima, N. Baboi, J. Bähr, and R. Brinkmann, Nat. Photon. **1**, 336 (2007).
8. M. Yamamoto and T. Namioka, Appl. Opt. **31**, 1622 (1992).
9. E. A. Vishnyakov, M. S. Luginin, A. S. Pirozhkov, E. N. Ragozin, and S. A. Startsev, Quantum Electron. **41**, 75 (2011).
10. I. V. Kozhevnikov, I. N. Bukreeva, and E. Ziegler, Nucl. Instr. Meth. Phys. Res. **460**, 424 (2001).
11. Y. Yao, H. Kunieda, H. Matsumoto, K. Tamura, and Y. Miyata, Appl. Opt. **52**, 6824 (2013).
12. Z. Wang, H. Wang, J. Zhu, Z. Zhang, Y. Xu, S. Zhang, and L. Chen, Appl. Phys. Lett. **90**, 031901 (2007).
13. R. Chen and F. Wang, Chin. Opt. Lett. **6**, 310 (2008).
14. M. Tan, H. Li, Q. Huang, H. Zhou, T. Huo, X. Wang, and J. Zhu, Chin. Opt. Lett. **9**, 023102 (2011).
15. J. Qin, J. Shao, K. Yi, and Z. Fan, Chin. Opt. Lett. **5**, 301 (2007).
16. Z. Wang, H. Wang, J. Zhu, Y. Xu, S. Zhang, C. Li, and L. Chen, Appl. Phys. Lett. **89**, 241120 (2006).
17. C. Montcalm, J. M. Slaughter, M. Chaker, P. A. Kearney, B. T. Sullivan, M. Ranger, and C. M. Falco, Opt. Lett. **19**, 1004 (1994).
18. B. Kjornrattanawanich and S. Bajt, Appl. Opt. **43**, 5955 (2004).
19. E. A. Vishnyakov, F. F. Kamenets, V. V. Kondratenko, M. S. Lugin, A. V. Panchenko, Y. P. Pershin, A. S. Pirozhkov, and E. N. Ragozin, Quantum Electron. **42**, 143 (2012).
20. D. Xu, Q. Huang, Y. Wang, P. Li, M. Wen, P. Jonnard, A. Giglia, I. V. Kozhevnikov, Z. Zhang, and Z. Wang, Opt. Express **23**, 33018 (2015).
21. Y. Wang, Q. Huang, Q. Yi, J. Zhang, M. Wen, J. Li, and Z. Wang, Proc. SPIE **9627**, 96271Q (2015).
22. C. Montcalm, P. A. Kearney, J. M. Slaughter, B. T. Sullivan, M. Chaker, H. Pépin, and C. M. Falco, Appl. Opt. **35**, 5134 (1996).
23. D. L. Windt and E. M. Gullikson, Appl. Opt. **54**, 5850 (2015).
24. K. D. Joensen, P. Gorenstein, J. Wood, F. E. Christensen, and P. Høghøj, Proc. SPIE **2279**, 180 (1994).
25. P. D. Binda and F. E. Zocchi, Proc. SPIE **5536**, 97 (2004).
26. I. V. Kozhevnikov, A. E. Yakshin, and F. Bijkerk, Opt. Express **23**, 9276 (2015).
27. B. L. Henke, E. M. Gullikson, and J. C. Davis, At. Data Nucl. Data Tables **54**, 181 (1993).
28. E. Spiller, *Soft X-Ray Optics* (SPIE Optical Engineering Press, 1994).
29. D. L. Windt, Comput. Phys. **12**, 360 (1998).
30. B. Kjornrattanawanich, "*Reflectance, Optical Properties, and Stability of Molybdenum/Strontium and Molybdenum/Yttrium Multilayer Mirrors*," Ph.D. Dissertation (University of California, 2002).